Novel hybrid three-dimensional artificial liver using human induced pluripotent stem cells and a rat decellularized liver scaffold

AUTHOR(S):

Minami, Takahito; Ishii, Takamichi; Yasuchika, Kentaro; Fukumitsu, Ken; Ogiso, Satoshi; Miyauchi, Yuya; Kojima, Hidenobu; ... Yasuda, Katsutaro; Osafune, Kenji; Uemoto, Shinji

CITATION:

Minami, Takahito ...[et al]. Novel hybrid three-dimensional artificial liver using human induced pluripotent stem cells and a rat decellularized liver scaffold. Regenerative therapy 2019, 10: 127-133

ISSUE DATE:

2019-06

URL:

http://hdl.handle.net/2433/243894

Regenerative Therapy 10 (2019) 127–133

Contents lists available at ScienceDirect

JSRM

Regenerative Therapy

journal homepage: http://www.elsevier.com/locate/reth

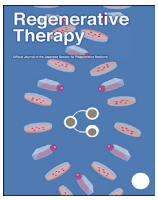

Original Article

Novel hybrid three-dimensional artificial liver using human induced pluripotent stem cells and a rat decellularized liver scaffold

Takahito Minami [a, b], Takamichi Ishii [a, *], Kentaro Yasuchika [a, c], Ken Fukumitsu [a], Satoshi Ogiso [a], Yuya Miyauchi [a], Hidenobu Kojima [a], Takayuki Kawai [a], Ryoya Yamaoka [a], Yu Oshima [a], Hiroshi Kawamoto [a], Maki Kotaka [b], Katsutaro Yasuda [a, b], Kenji Osafune [b], Shinji Uemoto [a]

[a] Department of Surgery, Graduate School of Medicine, Kyoto University, 54 Kawahara-cho, Shogoin, Sakyo-ku, Kyoto 606-8507, Japan
[b] Center for iPS Cell Research and Application (CiRA), Kyoto University, 53 Kawahara-cho, Shogoin, Sakyo-ku, Kyoto 606-8507, Japan
[c] Japanese Red Cross Wakayama Medical Center, 4-20 Komatsubara-dori, Wakayama City 640-8558, Japan

ARTICLE INFO

Article history:
Received 13 December 2018
Received in revised form
7 March 2019
Accepted 14 March 2019

Keywords:
Decellularized liver
Recellularization
Human iPSC
Hepatocyte
Artificial liver

ABSTRACT

Introduction: Liver transplantation is currently the only curative therapy for end-stage liver failure; however, establishment of alternative treatments is required owing to the serious donor organ shortage. Here, we propose a novel model of hybrid three-dimensional artificial livers using both human induced pluripotent stem cells (hiPSCs) and a rat decellularized liver serving as a scaffold.
Methods: Rat liver harvesting and decellularization were performed as reported in our previous studies. The decellularized liver scaffold was recellularized with hiPSC-derived hepatocyte-like cells (hiPSC-HLCs) through the biliary duct. The recellularized liver graft was continuously perfused with the culture medium using a pump at a flow rate of 0.5 mL/min in a standard CO_2 (5%) cell incubator at 37 °C.
Results: After 48 h of continuous perfusion culture, the hiPSC-HLCs of the recellularized liver distributed into the parenchymal space. Furthermore, the recellularized liver expressed the albumin (*ALB*) and *CYP3A4* genes, and secreted human ALB into the culture medium.
Conclusion: Novel hybrid artificial livers using hiPSCs and rat decellularized liver scaffolds were successfully generated, which possessed human hepatic functions.

1. Introduction

Liver transplantation is the only curative treatment for end-stage liver failure. However, the serious donor organ shortage presents a global problem. Although the need for alternative options for liver replacement, including bioartificial livers, is well recognized, the development of a transplantable artificial whole liver has not yet been realized, mainly owing to the difficulty of reproducing a complicated three-dimensional (3D) structure of native livers. Human induced pluripotent stem cells (hiPSCs) and human iPSC-derived hepatocyte-like cells (hiPSC-HLCs) are considered promising as suitable cell sources for alternative treatments of liver failure. However, the difficulty in constructing a transplantable 3D liver using hiPSCs or hiPSC-HLCs remains unsolved.

The recent development of a decellularization technique has now made it possible to construct an acellular 3D organ scaffold, including the heart [1], lung [2], liver [3, 4], and kidney [5]. A decellularized liver scaffold, which consists of an extracellular matrix (ECM) retaining the tissue-specific 3D ultrastructure, intact vascular networks for nutrient and gas transport, and molecules that may promote cell attachment and organ-specific differentiation of progenitor cells, is highly anticipated as a promising new material for whole-liver engineering by repopulating suitable hepatic cells, namely recellularization [6]. We have constructed an artificial recellularized liver with rat adult primary hepatocytes or mouse fetal primary hepatocytes, and evaluated their liver function [6, 7]. However, to our best knowledge, a recellularized artificial liver using hiPSCs has not yet been reported.

* Corresponding author. Fax: +81 75 751 4263.
E-mail address: taishii@kuhp.kyoto-u.ac.jp (T. Ishii).
Peer review under responsibility of the Japanese Society for Regenerative Medicine.

https://doi.org/10.1016/j.reth.2019.03.002

Thus, the aim of this study was to develop a novel artificial liver model using hiPSCs and rat decellularized liver scaffolds, and to evaluate its liver function.

2. Methods

2.1. Liver harvest and decellularization

Male Lewis rats (250–300 g; SLC, Hamamatsu, Japan) were used for liver harvesting and preparation of the decellularized liver scaffolds. All animal experimental protocols were approved by the Kyoto University Animal Experimentation Committee, and were performed in accordance with the Animal Protection Guidelines of Kyoto University.

Rat liver harvesting and decellularization were performed as reported in our previous studies [6–8]. The harvested livers were cannulated with a 24-gauge cannula in the biliary duct (BD) and a 20-gauge cannula in the portal vein (PV), and were stored in cell culture dishes with phosphate-buffered saline (PBS). The decellularization protocol is schematically summarized in Fig. 1. In brief, the livers were frozen at −80 °C and thawed at room temperature, followed by perfusion with 0.02% trypsin/0.05% EGTA solution through the PV for 1 h at 37 °C to detach cells from the ECM. Subsequently, a 1% Triton X-100/0.05% EGTA solution was perfused at 1 mL/min for 18–24 h until the livers were decellularized. The decellularized livers were then perfused with 0.1% peracetic acid for 2 h for sterilization, followed by perfusion with PBS.

2.2. hiPSCs culture

The experiments using hiPSCs were approved by the Ethics Committee of Kyoto University, and informed consent was obtained from the donors of hiPSCs.

The hiPSC cell line, 585A1 (Kyoto University, Japan), was maintained on feeder layers of mitomycin C-treated STO/Neo resistant/LIF (SNL) feeder cells in Primate ES medium (ReproCELL, Tokyo, Japan) with 4 ng/mL recombinant human basic fibroblast growth factor (Wako, Osaka, Japan) and 500 U/mL penicillin/streptomycin (PS; Thermo Fisher Scientific, Waltham, MA, USA). For routine passaging, hiPSC colonies were treated with dissociation solution consisting of 0.25% trypsin (Thermo Fisher Scientific), 0.1% collagenase IV (Thermo Fisher Scientific), 20% knockout serum replacement (KSR; Thermo Fisher Scientific), and 1 mM $CaCl_2$ in PBS (CTK dissociation solution), and split at a ratio between 1:8 and 1:12.

2.3. Differentiation of hiPSCs into hiPSC-HLCs

Differentiation protocols of hiPSCs into hiPSC-HLCs (Fig. 2) were based on our previous reports [9–11]. In brief, hiPSC colonies were treated with CTK dissociation solution. The cells were dissociated to single cells by mild pipetting after treatment with Accutase (Innovative Cell Technologies, San Diego, CA, USA) for 10–20 min and seeded on Matrigel-coated plates (Corning Incorporated, Corning, NY, USA) at a density of 1.0×10^5 cells/cm^2 with the stage 1 medium consisting of RPMI1640 (Nacalai Tesque, Kyoto, Japan) supplemented with 1 × B27 (Thermo Fisher Scientific), 500 U/mL PS, 100 ng/mL recombinant human/mouse/rat activin A (R&D Systems, Minneapolis, MN, USA), and 1 μM CHIR99021 (Axon Medchem, Groningen, the Netherlands). For the first day of differentiation culture, the ROCK inhibitor Y27632 (10 μM; Wako) was added to the medium to support cell survival, and then the cells were cultured for a total of 5–6 days. For stage 2, the cells were cultured in the stage 2 medium consisting of Knockout-Dulbecco's modified Eagle medium (Thermo Fisher Scientific), 20% KSR, 1 mM L-glutamine, 1% nonessential amino acids, 0.1 mM 2-mercaptoethanol, and 1% dimethyl sulfoxide (Sigma-Aldrich, St. Louis, MO, USA) for 6 days. For stage 3, the cells were cultured in the stage 3 medium consisting of hepatocyte culture medium (Lonza, Basel, Switzerland) supplemented with 20 ng/mL recombinant human hepatocyte growth factor (Peprotech, Rocky Hill, NJ, USA) and 20 ng/mL recombinant human oncostatin M (Peprotech) for 7–8 days.

2.4. Isolation of hiPSC-HLCs and recellularization of the decellularized liver scaffolds

The hiPSC-HLCs on stage 3, day 8 were dissociated by mild pipetting after treatment with Accumax (Innovative Cell Technologies) for 30 min at 37 °C, and the decellularized liver scaffolds were recellularized through the BD as we previously reported [6–8]. In brief, a decellularized liver scaffold was placed in a 100-mm culture dish and perfused with 20 mL of the stage 3 medium through the PV prior to recellularization. A total of 1.6×10^7 hiPSC-HLCs resuspended in 20 mL of the culture medium were introduced into the liver scaffold through the BD at a flow rate of 1 mL/min.

2.5. Perfusion culture of the recellularized liver grafts

Perfusion culture of the recellularized liver grafts was performed as we previously reported [6, 7]. In brief, after 3 h of static culture, the recellularized liver graft was transferred to a customized chamber for perfusion culture. The recellularized liver graft was connected to a recirculation circuit by a cannula inserted into the PV and continuously perfused with the stage 3 medium, using a Perista pump (ATTO, Tokyo, Japan) at a flow rate of 0.5 mL/min to prevent shear stress and mechanical damage to the engrafted cells (Fig. 3). The entire perfusion system was placed in a standard CO_2 (5%) cell incubator at 37 °C. As a control, perfusion culture of the decellularized liver graft without recellularization was also performed by using the same method.

2.6. Immunocytochemistry of hiPSC-HLCs

Immunocytochemistry of hiPSC-HLCs was performed as previously reported [12, 13]. Samples were incubated overnight at 4 °C with primary antibodies against SOX17 (1:100; R & D Systems, AF1924), HNF4a (1:50; Santa Cruz Biotechnology, Dallas, TX, USA, sc-374229), albumin (ALB; 1:500; Bethyl, Montgomery, TX, USA, A80-229A), alpha-fetoprotein (AFP; 1:500; Sigma-Aldrich A8452), and CYP3A4 (1:100; Proteintech, Rosemont, IL, USA, 18227-1-AP). After washing, the stained samples were incubated with Alexa 488-conjugated donkey anti-goat IgG (1:500; Thermo Fisher Scientific)

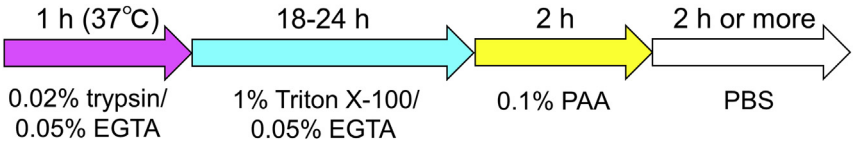

Fig. 1. Decellularization protocol of a rat whole liver.

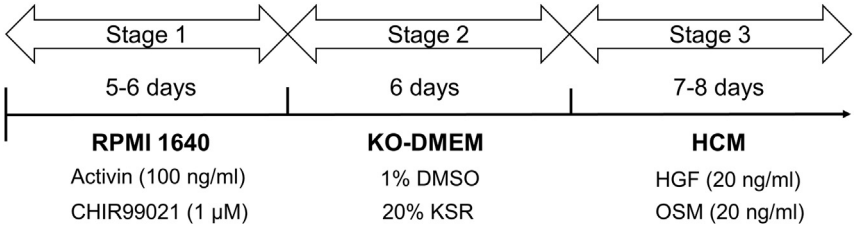

Fig. 2. Differentiation protocols of hiPSCs into hiPSC-HLCs.

for SOX17 or ALB, Alexa 488-conjugated donkey anti-rabbit IgG (1:200; Thermo Fisher Scientific) for CYP3A4, or Alexa 555-conjugated goat anti-mouse IgG (1:500; Thermo Fisher Scientific) for HNF4a or AFP detection. After washing, the samples were covered with Vectashield mounting medium containing 4,6-diamidino-2-phenylindole (DAPI) (Vector Laboratories, Burlingame, CA, USA). All samples were imaged using a BZ-9000 fluorescence microscope (Keyence, Osaka, Japan).

2.7. Histology and immunohistochemistry of decellularized liver scaffolds and recellularized liver grafts

Decellularized liver scaffolds and recellularized liver grafts were fixed with 4% paraformaldehyde, embedded in paraffin, and cut into 4-μm-thick sections. Hematoxylin and eosin (H&E) staining was performed according to standard protocols.

Immunofluorescent analyses were performed as reported previously [6, 7]. Antigen retrieval was achieved with a Target Retrieval Solution (Dako, Glostrup, Denmark). Non-specific binding was blocked with 1.4% bovine serum albumin (Sigma-Aldrich) dissolved in 0.1% saponin (Wako) in PBS. Sections were incubated overnight at 4 °C with primary antibodies of ALB, AFP, and CYP3A4. After washing, the stained sections were incubated with Alexa 488-conjugated donkey anti-goat IgG (1:500) for ALB, Alexa 488-conjugated donkey anti-rabbit IgG (1:200) for CYP3A4, or Alexa 555-conjugated goat anti-mouse IgG (1:500) for AFP detection for 2 h at room temperature. After washing, the stained sections were covered with Vectashield mounting medium containing DAPI. All samples were imaged using a BZ-9000 fluorescence microscope (Keyence).

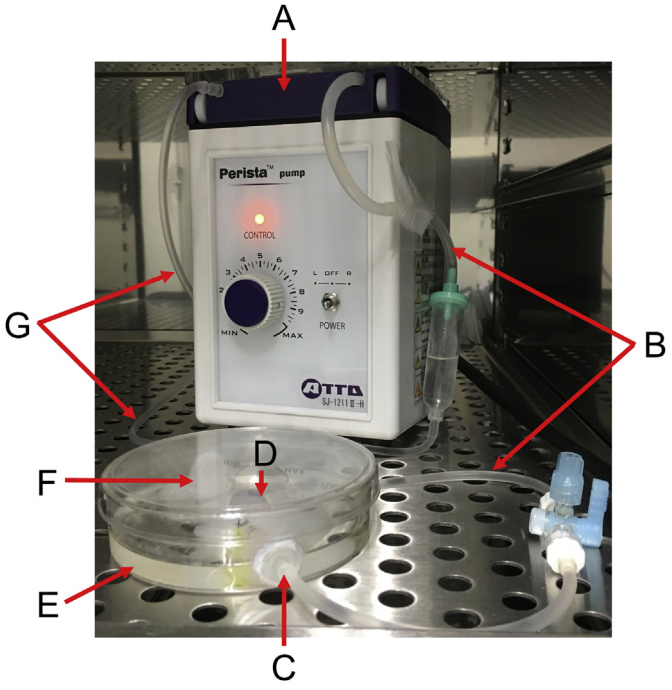

Fig. 3. The recellularized liver graft (RL) was connected to the recirculation circuit by a cannula inserted into the PV, and continuously perfused with the culture medium using a Perista pump. (A) Pump continuously perfusing the culture medium. (B) Inflow into RL. (C) Connection port into the PV cannula of RL. (D) RL. (E) Culture medium. (F) Aspiration port of the culture medium in the culture dish. (G) Outflow from the culture dish.

2.8. Reverse transcription polymerase chain reaction (RT-PCR)

Total RNA was extracted from the recellularized hiPSC-HLCs after 48 h of perfusion culture using a Pure Link RNA Mini Kit (Invitrogen), and 200 ng of total RNA was reverse-transcribed to cDNA using ReverTra Ace (TOYOBO, Osaka, Japan) according to the manufacturer protocols. The following primers were amplified: *HNF4a* forward 5′–CCAAGTACATCCCAGCTTTC, reverse 5′-TTGGCATCTGGGTCAAAG; *ALB* forward 5′-TGGGCAGCAAATGTTGTAAA, reverse 5′-CTCCTTATCGTCAGCCTTGC; and *CYP3A4* forward 5′–CCTTACACATACACACCCTTTGGAAGT, reverse 5′-AGCTCAATGCATGTACAGAATCCCCGGTTA. RT-PCR was performed as previously described [13–15]. RT-PCR was also performed for hiPSCs and hiPSC-HLCs at stage 3, day 8 in the same manner.

2.9. Evaluation of recellularized liver function

The culture medium of the recellularized liver graft and decellularized liver graft was collected after 48 h of perfusion, and the human ALB content was measured using the human albumin enzyme-linked immunosorbent assay quantitation kit (Bethyl) according to the manufacturer's protocol. The human ALB content in the medium of undifferentiated hiPSCs and hiPSC-HLCs at stage 3, day 8 *in vitro* was also measured by using the same method.

2.10. Statistical analysis

Data are expressed as mean ± standard error of mean. Statistical analysis was performed using GraphPad Prism for Windows, version 6.0 (GraphPad Software, La Jolla, CA, USA). Statistical significance was defined as $p < 0.05$. The cumulative human albumin production of each group was compared using Student's t-test with Bonferroni correction.

3. Results

3.1. Decellularization of the whole liver

A translucent acellular liver scaffold was obtained after 24 h of the decellularization procedure (Fig. 4A). Histological analysis of the decellularized liver scaffold confirmed the lack of nuclei or cytoplasmic components in the scaffolds (Fig. 4A). Crystal violet

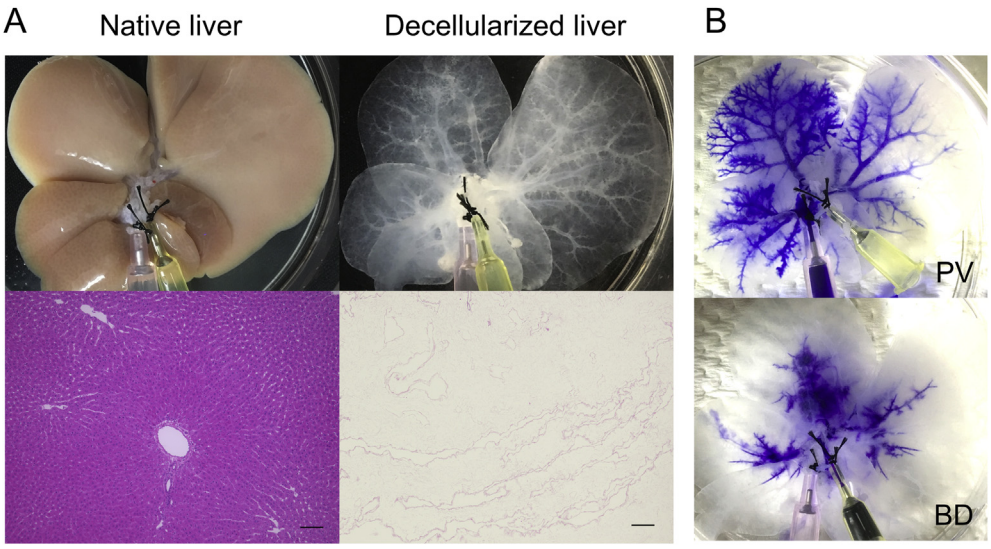

Fig. 4. Preparation of the rat decellularized whole liver scaffold and evaluation of the seeding or perfusion route. (A) Macroscopic and histological comparison of rat native (left panels) and decellularized livers (right panels). H&E staining showed no remaining nuclei or cytoplasmic components in the scaffolds (lower right panel). Scale bars: 100 μm. (B) Crystal violet staining of the intrahepatic portal vein (PV; upper panel) and biliary duct (BD; lower panel) demonstrated their patency.

staining further showed that the PV and BD were intact after the decellularization (Fig. 4B), allowing for recellularization and perfusion culture.

3.2. Immunocytochemical evaluation of hiPSC-HLCs

Immunofluorescent staining showed that the hiPSC-HLCs expressed liver-related markers, including SOX17 at stage 1, day 6 (Fig. 5A), HNF4a and AFP at stage 2, day 6 (Fig. 5B), and ALB, AFP, and CYP3A4 at stage 3, day 8 (Fig. 5C). These findings confirmed that the hiPSC-HLCs showed hepatocyte-like characteristics.

3.3. Macroscopic and histological observations of the liver recellularized with hiPSC-HLCs

Macroscopic observation of the recellularized liver showed that hiPSC-HLC clusters were broadly distributed in the liver lobe (Fig. 6A). H&E staining of the recellularized liver after 48 h of perfusion culture demonstrated that the vascular structures were intact, and the hiPSC-HLCs were distributed into the parenchymal space (Fig. 6B). The cell array was similar to that of epithelial cells, and the cell structure, including nuclei or cytoplasm, was retained (Fig. 6C and D).

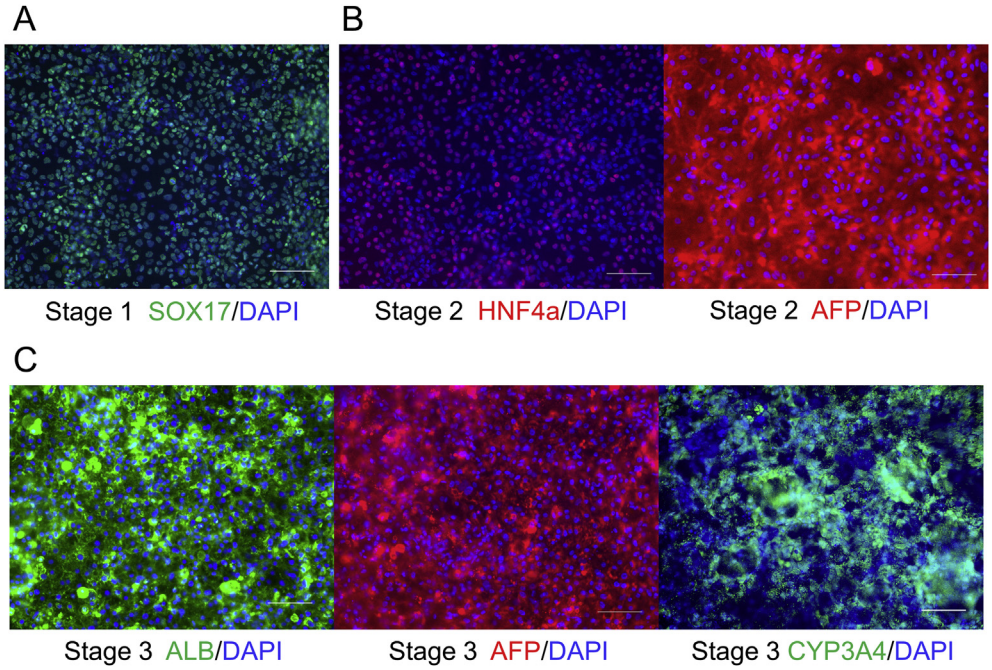

Fig. 5. Immunostaining analysis demonstrated hepatic differentiation of hiPSCs into hiPSC-HLCs *in vitro*. (A) SOX17 (green) expression at stage 1, day 6. (B) HNF4a (red) and AFP (red) expression at stage 2, day 6. (C) Albumin (ALB; green), AFP (red), and CYP3A4 (green) expression at stage 3, day 8. Scale bars: 100 μm. In all figures, blue fluorescence indicates DAPI.

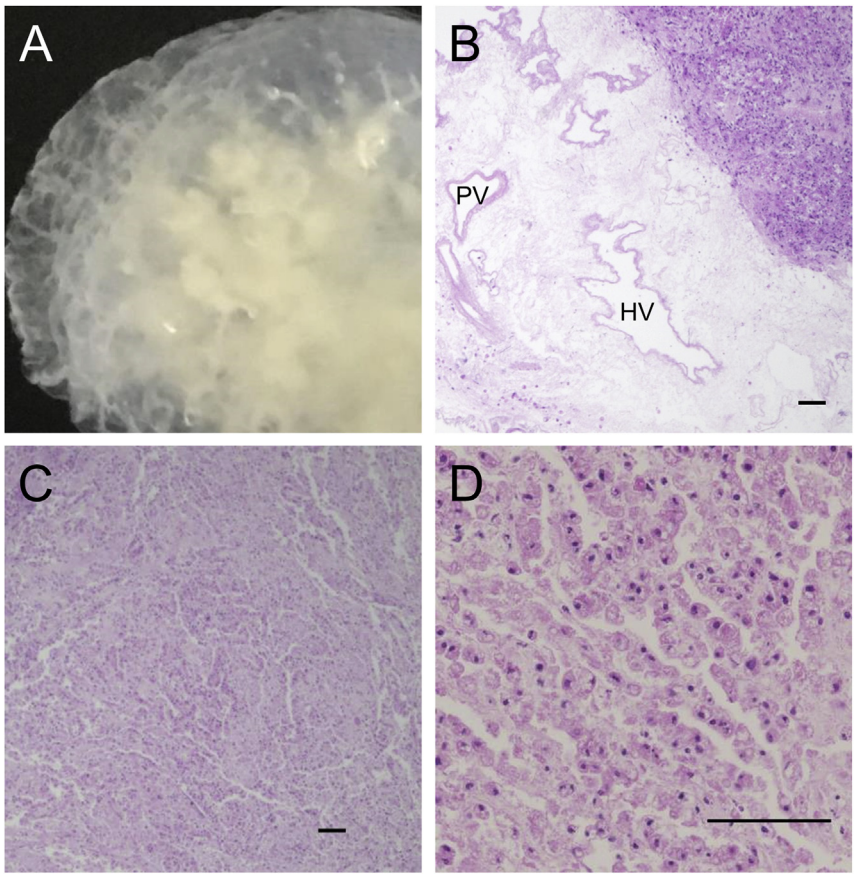

Fig. 6. Macroscopic and H&E staining observation of the liver graft recellularized with hiPSC-HLCs after 48 h of perfusion culture. Macroscopic observation of the recellularized liver showed that hiPSC-HLC clusters widely spread in the liver lobe (A). The cells were distributed into the parenchymal space, and the portal vein (PV) and hepatic vein (HV) were intact (B). The cell array was similar to that of epithelial cells, and the cell structures, including nuclei or cytoplasm, were retained (C, D). Scale bars: 100 μm.

3.4. Evaluation of hepatic function of the recellularized liver graft

Immunofluorescent staining of the recellularized liver after 48 h of perfusion culture showed that hiPSC-HLCs seeded through the BD expressed liver-related markers, including ALB, AFP, and CYP3A4 (Fig. 7A). RT-PCR analysis demonstrated the mRNA expression of *HNF4a*, *ALB*, and *CYP3A4* in the hiPSC-HLCs following 48 h of perfusion culture in the recellularized liver. The mRNA expression level of *CYP3A4* in the recellularized liver after 48 h of perfusion culture appeared to be higher than that in the hiPSC-HLCs at stage 3, day 8 *in vitro* (Fig. 7B). The cumulative human ALB secretion in the recellularized livers after 48 h of perfusion culture was 31.34 ± 16.82 ng/10^6 cells, whereas the cumulative human ALB secretion of hiPSC-HLCs at stage3, day8 *in vitro* for 48 h was 172.0 ± 12.03 ng/10^6 cells ($p < 0.05$). The cumulative human ALB secretion in the decellularized liver after 48 h of perfusion culture and undifferentiated hiPSCs was undetectable (Fig. 7C).

4. Discussion

In this study, we successfully developed a novel artificial liver model using hiPSCs and a rat decellularized liver scaffold, and demonstrated its potential for human liver function. RT-PCR and immunofluorescence analysis showed the expression of human ALB and CYP3A4 in the recellularized liver. Moreover, ELISA revealed that the recellularized liver secreted human ALB. These results suggest that the 3D artificial livers generated in this study have human liver-characteristic function, including the secretion of liver-related proteins or drug metabolism. Functional recellularized livers with non-human iPSCs have been reported previously [16]; however, to our best knowledge, this is the first study to generate a recellularized liver model with human hepatic function using hiPSCs.

On the other hand, the fact that AFP was still expressed in the recellularized liver suggested that the hiPSC-HLCs in the recellularized liver after perfusion culture were not sufficiently mature. The ALB secretion ability of the recellularized livers was approximately 1/5 to 1/6 that of hiPSC-HLCs *in vitro*, and 1/70 to 1/100 that of the liver recellularized with adult rat primary hepatocytes [6, 7]. We speculated that this was because the procedure of isolating hiPSC-HLCs before recellularization might cause cell damage and decrease hepatocyte function. Moreover, bile production in the recellularized liver was not confirmed. These deficiencies could result in unsatisfactory hepatic functions of the recellularized liver graft with hiPSC-HLCs, which is a limitation of the current method that should be overcome with optimization of the protocol in further studies.

Xenogeneic decellularized scaffolds have been reported to show low immunogenicity [17]; thus, decellularized liver scaffolds derived from other species could be suitable for human organ transplantation without the risk of severe immune rejection. Furthermore, the decellularized scaffold retained its intact vascular structure. Thus, the decellularized organs can be transplanted *in vivo* by vascular anastomosis as well as through current transplant surgical methods. This is the main advantage of artificial liver engineering using a decellularized scaffold in comparison with micro-3D liver buds derived from hiPSCs [18, 19]. We previously reported that

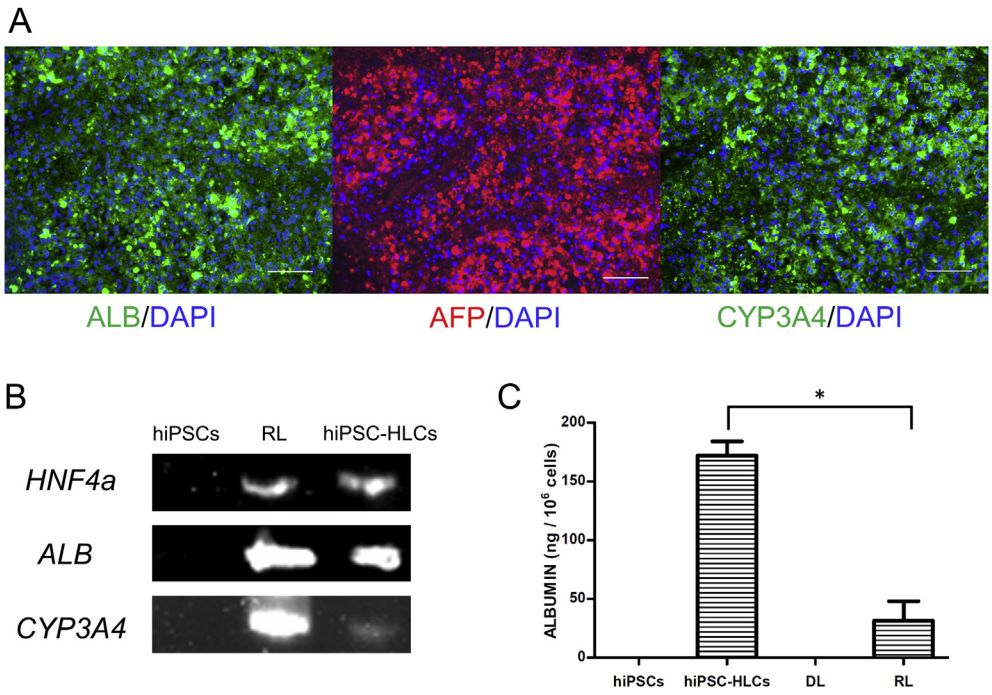

Fig. 7. Evaluation of hepatic function of the recellularized liver graft after the 48 h perfusion culture. (A) Immunostaining analysis: albumin (ALB; green), AFP (red), and CYP3A4 (green). Scale bars: 100 μm. Blue fluorescence indicates DAPI. (B) RT-PCR analysis for *HNF4a*, *ALB*, and *CYP3A4*. The left lane indicates hiPSCs, the middle lane shows the recellularized liver (RL), and the right lane indicates the hiPSC-HLCs at stage 3, day 8 *in vitro* (hiPSC-HLCs). (C) Cumulative human albumin secretion in hiPSC-HLCs at stage 3, day 8 *in vitro* (hiPSC-HLCs), and the recellularized liver graft (RL). Error bars represent standard error of mean (SEM; n = 3, $^*p < 0.05$). Cumulative human albumin secretion in undifferentiated hiPSCs (hiPSCs) and the decellularized liver graft (DL) was undetectable (n = 3).

rat primary hepatocytes could be more efficiently distributed into the parenchymal space of the decellularized liver through the BD, rather than through the PV [6]. Thus, in the present study, the hiPSC-HLCs were injected into the decellularized liver scaffolds through the BD, and the hiPSC-HLCs were distributed and engrafted in the parenchymal space of the rat decellularized livers. This result suggested that the BD was an appropriate recellularization pathway regardless of the hepatocyte type. For transplantable liver engineering in the future, recellularization through the BD might be very advantageous because the PV remains intact; moreover, re-endothelialization of the PV could be performed to prevent thrombogenesis, which would also maintain the blood perfusion of artificial livers. We have previously reported that re-endothelialization using rat primary liver sinusoidal endothelial cells maintained the hepatic function of the recellularized liver with rat primary hepatocytes, and supported hepatocyte viability under blood perfusion in the recellularized liver graft owing to their antithrombogenicity [7]. Re-endothelialization using human-derived endothelial cells and co-culture with hiPSC-HLCs still presents several challenges, which should be addressed in future studies.

5. Conclusion

We successfully developed a novel artificial liver model using hiPSCs and a rat decellularized liver scaffold. This hybrid liver model with human liver function could open the door to develop entirely non-antigenic transplantable artificial livers utilizing autologous hiPSCs derived from the patients themselves.

Acknowledgements

This work was supported by Japan Society for the Promotion of Science (Grant Number: 16H05489).

The authors would like to thank Dr. Ben Sasaki (Department of Life Science Frontiers, Center for iPS Cell Research and Application, Kyoto University, Kyoto, Japan) for helpful technical support.

Conflicts of interest

K.O. is a founder and a member without salary of the scientific advisory boards of iPS Portal Japan.

Appendix A. Supplementary data

Supplementary data to this article can be found online at https://doi.org/10.1016/j.reth.2019.03.002.

References

[1] Ott HC, Matthiesen TS, Goh SK, Black LD, Kren SM, Netoff TI, et al. Perfusion-decellularized matrix: using nature's platform to engineer a bioartificial heart. Nat Med 2008;14:213–21.
[2] Ott HC, Clippinger B, Conrad C, Schuetz C, Pomerantseva I, Ikonomou L, et al. Regeneration and orthotopic transplantation of a bioartificial lung. Nat Med 2010;16:927–33.
[3] Uygun BE, Soto-Gutierrez A, Yagi H, Izamis ML, Guzzardi MA, Shulman C, et al. Organ reengineering through development of a transplantable recellularized liver graft using decellularized liver matrix. Nat Med 2010;16:814–20.
[4] Baptista PM, Siddiqui MM, Lozier G, Rodriguez SR, Atala A, Soker S. The use of whole organ decellularization for the generation of a vascularized liver organoid. Hepatology 2011;53:604–17.
[5] Song JJ, Guyette JP, Gilpin SE, Gonzalez G, Vacanti JP, Ott HC. Regeneration and experimental orthotopic transplantation of a bioengineered kidney. Nat Med 2013;19:646–51.
[6] Ogiso S, Yasuchika K, Fukumitsu K, Ishii T, Kojima H, Miyauchi Y, et al. Efficient recellularisation of decellularised whole-liver grafts using biliary tree and foetal hepatocytes. Sci Rep 2016;6:35887.
[7] Kojima H, Yasuchika K, Fukumitsu K, Ishii T, Ogiso S, Miyauchi Y, et al. Establishment of practical recellularized liver graft for blood perfusion using primary rat hepatocytes and liver sinusoidal endothelial cells. Am J Transplant 2018;18:1351–9.

[8] Miyauchi Y, Yasuchika K, Fukumitsu K, Ishii T, Ogiso S, Minami T, et al. A novel three-dimensional culture system maintaining the physiological extracellular matrix of fibrotic model livers accelerates progression of hepatocellular carcinoma cells. Sci Rep 2017;7:9827.
[9] Kajiwara M, Aoi T, Okita K, Takahashi R, Inoue H, Takayama N, et al. Donor-dependent variations in hepatic differentiation from human-induced pluripotent stem cells. Proc Natl Acad Sci U S A 2012;109:12538–43.
[10] Kotaka M, Toyoda T, Yasuda K, Kitano Y, Okada C, Ohta A, et al. Adrenergic receptor agonists induce the differentiation of pluripotent stem cell-derived hepatoblasts into hepatocyte-like cells. Sci Rep 2017;7:16734.
[11] Yoshitoshi-Uebayashi EY, Toyoda T, Yasuda K, Kotaka M, Nomoto K, Okita K, et al. Modelling urea-cycle disorder citrullinemia type 1 with disease-specific iPSCs. Biochem Biophys Res Commun 2017;486:613–9.
[12] Ishii T, Yasuchika K, Fujii H, Hoppo T, Baba S, Naito M, et al. In vitro differentiation and maturation of mouse embryonic stem cells into hepatocytes. Exp Cell Res 2005;309:68–77.
[13] Kawai T, Yasuchika K, Ishii T, Katayama H, Yoshitoshi EY, Ogiso S, et al. Keratin 19 , a cancer stem cell marker in human hepatocellular carcinoma. Clin Cancer Res 2015;21:3081–91.
[14] Yamaoka R, Ishii T, Kawai T, Yasuchika K, Miyauchi Y, Kojima H, et al. CD90 expression in human intrahepatic cholangiocarcinoma is associated with lymph node metastasis and poor prognosis. J Surg Oncol 2018;118:664–74.
[15] Katayama H, Yasuchika K, Miyauchi Y, Kojima H, Yamaoka R, Kawai T, et al. Generation of non-viral, transgene-free hepatocyte like cells with piggyBac transposon. Sci Rep 2017;7:44498.
[16] Park KM, Hussein KH, Hong SH, Ahn C, Yang SR, Park SM, et al. Decellularized liver extracellular matrix as promising tools for transplantable bioengineered liver promotes hepatic lineage commitments of induced pluripotent stem cells. Tissue Eng Part A 2016;22(5-6):449–60.
[17] Mirmalek-Sani SH, Sullivan DC, Zimmerman C, Shupe TD, Petersen BE. Immunogenicity of decellularized porcine liver for bioengineered hepatic tissue. Am J Pathol 2013;183:558–65.
[18] Takebe T, Sekine K, Enomura M, Koike H, Kimura M, Ogaeri T, et al. Vascularized and functional human liver from an iPSC-derived organ bud transplant. Nature 2013;499:481–4.
[19] Takebe T, Zhang RR, Koike H, Kimura M, Yoshizawa E, Enomura M, et al. Generation of a vascularized and functional human liver from an iPSC-derived organ bud transplant. Nat Protoc 2014;9:396–409.